ORIENTAL JOURNAL OF CHEMISTRY
An International Open Access, Peer Reviewed Research Journal
www.orientjchem.org
ISSN: 0970-020 X
CODEN: OJCHEG
2026, Vol. 42, No.(2):
Pg. 428-438

Study Using a Mixed Full Factorial Design of the Effects of Matrix–Reinforcement Interactions on the Mechanical and Optical Properties of Starch-Based Bioplastics

OUATTARA TANIKY SY HAMED[1], YACOUBA ZOUNGRANAN[1, 2*], SÉVÉRIN N'GORAN EROI[1], KAGA TABA TO'ORA[3] ,EKOU LYNDA[1] and EKOU TCHIRIOUA[1]

[1]Laboratory of Thermodynamics and Environmental Physical Chemistry, Nangui ABROGOUA University 02 BP 802 Abidjan 02, Côte d'Ivoire,
[2]Department of Mathematics, Physics, and Chemistry, Peleforo GON COULIBALY University. B.P. 1328, Korhogo, Côte d'Ivoire
[3]Water and Environment Laboratory Limoges E2Lim, UR 24133, ENSIL-ENSCI, University of Limoges, France
*Corresponding author E-mail: zoungranan@gmail.com

http://dx.doi.org/10.13005/ojc/420206

(Received: February 28, 2026; Accepted: April 06, 2026)

ABSTRACT

Bioplastics offer an alternative to conventional petrochemical-based plastics. This type of plastic has many advantages. However, when synthesized from bioresources without the addition of reinforcing agents, they exhibit poor mechanical and optical performance; it is therefore necessary to incorporate reinforcing agents to improve their properties. In this study, a mixed full factorial design (2^3) was applied by combining three continuous factors (CNF-Raw, CNF-Alkaline, CNC) and a four-level categorical factor corresponding to the oxidized starch matrices (Oxpot, Oxyam, Oxcas, Oxcor). The results showed that the Oxyam matrix (D_2) potentiates the effect of the fibers, simultaneously improving the breaking strength (R_1), elongation at break (R_2), and opacity (R_3) of the films. The D_2X_1 interaction revealed a notable synergy between the matrix and the reinforcements, regardless of the response obtained. The results also showed that Test 26 offers a satisfactory balance between the mechanical and optical properties of the TPS film. The values obtained for R_1, R_2, and R_3 were 95.3 MPa, 17.06%, and 17.56%, respectively. SEM analysis revealed the presence of microcracks and scattered, unconnected discontinuities in the film's internal structure

Keywords : Bioplastics, Starch, Design of experiments, Mechanical properties.

INTRODUCTION

Plastic is ubiquitous in everyday life, from food packaging to the manufacture of our electronic devices. It is a lightweight, inexpensive, and versatile material. In 2023, global plastic production was estimated at 413.8 million tons, 90.4% of which was derived from fossil fuels or petrochemicals [1]. Among the possible uses of plastics, packaging accounts for the largest share and is expected to reach approximately 30% of the total over the next 40 years [2]. Petrochemical plastics therefore account for nearly all plastics currently used in developing countries. This type of plastic has low biodegradability, making it persistent in the environment. Furthermore, it often contains toxic substances that can harm animal and human health. It is therefore necessary to find alternatives to petrochemical-based plastics. It is in this context that bioplastics emerge as a credible, sustainable, and innovative alternative [3]. Generally derived from bioresources such as starch, cellulose, or plant proteins, among others, bioplastics offer the advantage of being highly biodegradable and having a reduced carbon footprint. Among the available bioresources, starch remains the most studied biopolymer by the scientific community due to its abundance, low cost, and ability to be converted into thermoplastic material [4,5]. However, starch-based bioplastics still have significant limitations, notably insufficient mechanical strength, poor dimensional stability, and variable optical properties, which restrict their industrial applications. To address these shortcomings, many recent studies have focused on incorporating lignocellulosic reinforcements, such as plant fibers, cellulosic fillers, or agricultural byproducts. These reinforcements improve the stiffness, mechanical strength, and sometimes the transparency of starch-based bioplastics, thanks to the formation of effective interfacial interactions between the starch matrix and the intrinsic structure of the reinforcement [6]. A high-quality bioplastic is a material that exhibits good mechanical and optical properties and is readily biodegradable. These properties are closely linked to the mixture of reactants during bioplastic synthesis (starches, reinforcements, plasticizers, etc.). It is therefore necessary to determine, during synthesis, the factors likely to influence the mechanical, optical, and biodegradability properties of the bioplastic. In this study, the design of experiments (DOE) methodology was used as a statistical tool to systematically analyze the influence of several factors and their interactions on the final properties of the bioplastics. Four types of pre-oxidized starches (Oxpot, Oxcas, Oxyam, and Oxcor) were enriched with coconut fibers (raw, modified, and nanocellulosic). For each type of starchy biomass, three types of reinforcements were applied, and the mechanical and optical properties of the resulting bioplastics were evaluated. To do this, a 4×2^3 mixed factorial design was applied. The type of biomass was considered a four-level categorical factor, combined with three other continuous factors (CNF_Brute, CNF_Alkaline, and cellulose nanocrystals) at two levels. The objective was to primarily examine the influence of the type of biomass on the mechanical and optical properties of the resulting bioplastics.

MATERIALS AND METHODS

Study Materials

In our previous work [7], native starches were extracted from yam tubers (*Dioscorea alata L.*), sweet potatoes (*Ipomoea batatas*), cassava (*Manihot esculenta Crantz*), and corn kernels (*Zea mays saccharata*), designated Yam, Pot, Cas, and Cor, respectively. Optimal oxidation of the native starches was achieved using hydrogen peroxide ($H^2O^2_2$) concentrations of 1, 0.2, 0.6, and 0.6 M. In the present study, native starches oxidized with $H^2O^2_2$ were used as base matrices. Mature coconuts (*Cocos nucifera*), rich in lignocellulosic fibers, were harvested in Abidjan in the municipality of Port-Bouët ($5°15_225_2$ N; $3°57_231_2$ W).

Preparation of Reinforcements. Obtaining Fibers from (*Cocos nucifera)*

The extraction of raw coconut fibers (Cocos nucifera) was performed according to the method described in [8], with slight modifications. The raw lignocellulosic fibers were manually extracted from the mesocarp of *Cocos nucifera* coconuts. The fibers were washed with tap water, then thoroughly rinsed with distilled water and pre-dried at room temperature for 5 hours, then placed in an oven (Memmert, Germany) at 105°C for 24 hours. After drying, the fibers were ground using a laboratory grinder (Silver Crest, professional blender), then sieved using a sieve (Saulas, Paris) with a mesh diameter of 160 µm. The resulting sieved material

represents the raw coconut fibers (*Cocos nucifera*) Raw *Cocos nucifera* coconuts Fiber (CNF-Raw) (Figure 1) used in the study.

Preparation of Alkaline-Modified Fibers from *(Cocos nucifera)*

The preparation of alkaline-modified fibers was carried out based on the method described in the literature[9], with some modifications. The Cocos nucifera nuts were thoroughly washed, and then the fibrous part (mesocarp) was manually separated from the shell by peeling. The resulting mesocarps were subjected to an alkaline treatment to remove non-cellulosic compounds. To do this, the fibers were completely immersed in a 17.5% aqueous NaOH solution, at a solid-to-liquid ratio of 3 g/500 mL, and then kept under agitation at 80 °C for 4 hours using a heated magnetic stirrer (IKA RET-GS, Germany). Following the treatment, the fibers were thoroughly washed with distilled water until the pH reached neutral to remove alkaline residues, then dried at 105 °C for 24 hours in an oven (Memmert, Germany). The dry fibers were then ground and sieved using a sieve (Saulas, Paris) with a mesh size of 160 µm. The resulting sieved material represents the alkalized fibers (CNF_Alkaline) (Figure 2) in this study.

Extraction of cellulose nanocrystals (CNC)

Cellulose nanocrystals (CNC) were prepared by acid hydrolysis using the adapted method[10] with modifications. The Cocos nucifera fibers (mesocarp) were first subjected to an alkaline treatment designed to remove surface impurities and promote swelling of the cellulose walls. To this end, 10 g of fibers were immersed in 100 mL of a mol·L_2^1 NaOH solution and stirred at 750 rpm for 6 h at room temperature using a heated magnetic stirrer (IKA RET-GS, Germany). The fibers were then rinsed with distilled water (Milli-Q, 18 MΩ·cm) until the pH was neutral, then dried at 105 °C for 24 h in an oven (Memmert, Germany). The alkali-treated fibers were bleached by oxidative treatment in a 6% hydrogen peroxide ($H^2O^2_2$) solution, in the presence of a few drops of glacial acetic acid to maintain a slightly acidic pH (5–6), until homogeneous bleached fibers were obtained. After washing with distilled water (Milli-Q, 18 MΩ·cm) until pH neutral, a second drying was performed at 105 °C for 24 h (Memmert, Germany). Acid hydrolysis was performed by dispersing 5 g of bleached fibers in 500 mL of a 64% sulfuric acid solution. The mixture was kept under agitation at 80 °C for 4 h at 750 rpm using a magnetic stirrer (IKA RET-GS, Germany), resulting in the formation of a whitish paste. The reaction was stopped by dilution with 1 L of distilled water. The resulting suspension was washed until pH neutral, then centrifuged at 4,000 rpm for 30 min (centrifuge, Sigma-Aldrich, France); this step was repeated until the supernatant stabilized. The suspension was then vacuum-filtered until pH = 7. Finally, the final paste was dried at 105 °C in a universal oven (Memmert, Germany), then ground using a porcelain mortar with a beak (25 mL, D = 60 × 32 mm) equipped with a 52 mm pestle and sieved using a 100 µm sieve (Caulas, France) to obtain a fine white powder of cellulose nanocrystals (CNC) (Figure 3).

General Methodology for the Synthesis of Bioplastics

The bioplastics were prepared according to the method described in the literature[11], with minor modifications. A mass of m_a = 2.5 g of oxidized starch was dispersed in a beaker (250 mL), followed by the successive addition of the reinforcing agent (mf), water (Veau), glycerol (Vg), and an HCl solution (0.1 M; VHCl). The mixture was homogenized manually and then heated to 80 °C on a hot plate (IKA RET-GS, Germany) under continuous stirring for a period of time (t_i). To maintain a viscosity compatible with stirring, a volume (V_{NaOH}) of NaOH (0.1 M) was added as needed. Heating was continued until a homogeneous, viscous, and translucent matrix was obtained. The formulation was then poured onto cooled glass plates and dried at room temperature for 120 h. The formed films were peeled off manually and packaged for characterization.

Properties of the Bioplastics

Characterization tests are necessary to evaluate the mechanical and optical properties of the synthesized bioplastics.

Mechanical Properties

Two mechanical characterization tests were performed. The breaking strength (R_1) and elongation at break (R_2) of the films were determined using a universal tensile testing machine (Instron 5967, Instron, USA) equipped with a 30 kN load cell. The tests were performed on standard Type IV specimens (Figure 4) in accordance with ASTM

D-638, featuring a dumbbell-shaped geometry. The tensile speed was 5 mm·min^{-1}. The machine continuously recorded force and displacement, allowing for the calculation of the tensile strength at break $_2r$ (MPa) and the elongation at break (%). Each film was tested in triplicate

Optical response: measurement of opacity

A UV-VIS spectrophotometer was used to measure the opacity (R_3) of the bioplastic films. For each type of bioplastic, a 1.5 cm x 1.5 cm sample was carefully placed in the spectrophotometer cuvette to measure optical density at 600 nm. The measurement was performed in triplicate, and opacity was determined using the following equation 1:

$$\boldsymbol{Opacity}\ (\%) = \frac{\boldsymbol{A^{600\ nm}}}{\boldsymbol{X}} \times \mathbf{100} \qquad ...(1)$$

Where: A_{600nm}: Absorbance at 600 nm, X: film thickness (cm) determined using a digital caliper.

Description of the mixed full factorial design of the study

A mixed full factorial design was implemented to evaluate the combined effect of quantitative and qualitative factors on three bioplastic properties: breaking strength (R_1), elongation at break (R_2), and opacity (R_3). These three responses will allow us to better characterize the mechanical and optical properties of the bioplastics. Three continuous factors related to the mass of the reinforcements were selected: $X_1 = m_{(CNF\text{-}Raw)}$, $X_2 = m_{(CNF\text{-}Alkaline)}$, and X_3 = m(CNC), each studied at two coded levels (–1, +1). A categorical factor Di, related to the type of oxidized starch matrix or the nature of the matrix, was used. This categorical factor comprises four fixed-mass modalities (ma = 2.5 g) for each type of starch (D_1 = Oxpot, D_2 = Oxyam, D_3 = Oxcas, and D_4 = Oxcor). The combination of these factors resulted in a (4×2^3) design, comprising 32 trials conducted under identical conditions, allowing for the simultaneous exploration of main effects and interactions. The non-essential controllable operating parameters were determined based on preliminary trials. These include the volume of water (V_{water} = 80 mL), the volume of hydrochloric acid (V_{HCl} = 1 mL), the volume of sodium hydroxide (V_{NaOH} = 1 mL), the volume of glycerol (V_g = 2 mL), and the heating time (5 min) at room temperature. The experimental design is shown in Table 1, and the experimental matrix and responses are shown in Table 2. All data were analyzed using JMP software (version 13). ANOVA was used to assess the significance of effects and interactions, with a threshold of $p < 0.05$, to identify the factors influencing the optical and mechanical properties of the bioplastics.

A full mixed factorial design with four factors was used to determine the tensile at break ($_2r$)(R1), elongation at break (R2), and opacity (R3) of the bioplastics; the results are presented in Table 2. The behavior of these experimental responses was described using a first-order polynomial model (equation 2), incorporating the main effects, two-way interactions between the studied factors, and the influence of the categorical factor related to the matrix :

$$\boldsymbol{R_{general}} = b_0 + b_1X_1 + b_2X_2 + b_3X_3 + b_{12}X_1X_2 + b_{13}X_1X_3 + b_{23}X_2X_3 + \sum_{m=1}^{4} b_{0_m}D_m + b_{1_m}X_1D_m + b_{2_m}X_2D_m + b_{3_m}X_3D_m \qquad (2)$$

Scanning Electron Microscopy (SEM) Analysis

Morphological observations of the film were performed using a Hitachi TM3000 scanning electron microscope (SEM) (Model Name: TM3000, Serial Number: 103121-08, Data Number: 187 3R QRS0097). A small amount of each sample was deposited by pressing onto a conductive carbon pad and then placed in the microscope's observation chamber. The analyses were performed at a fixed acceleration voltage of 15 kV.

Data processing

All calculations and graphs were generated using Origin Pro 2024. The mean values and standard deviation were determined from three individual measurements.

RESULTS AND DISCUSSION

Analysis of results from the mixed full factorial design.

Presentation of responses and models

The various responses from the first-order polynomial model are given by the equations below: strength at break: R_1

$$R_1^{(D1)} = 69.071875 + 72.425X_1 + 80.075X_2 + 66.075X_3 - 610.2X_1X_2 - 233.4X_1X_3 - 40.325D_1X_1 - 14.575D_1X_2 - 18.175\ D_1X_3 \qquad (3)$$

$$R_1^{(D2)} = 69.071875 + 72.425X_1 + 80.075X_2 + 66.075X_3 - 610.2X_1X_2 - 233.4X_1X_3 - 201X_2X_3 + 82.875\ D_2X_1 + 26.825D_2X_2 - 39.975\ D_2X_3 \quad (4)$$

$$R_1^{(D3)} = 69.071875 + 72.425X_1 + 80.075X_2 + 66.075X_3 - 610.2X_1X_2 - 233.4X_1X_3 - 201X_2X_3 - 0.125D_3X_1 + 27.825D_3X_2 + 23.425D_3X_3 \quad (5)$$

$$R_1^{(D4)} = 69.071875 + 72.425X_1 + 80.075X_2 + 66.075X_3 - 610.2X_1X_2 - 233.4X_1X_3 - 201X_2X_3 - 42.425\ D_4X_1 - 40.075\ D_4X_2 - 40.075D_4X_3 \quad (6)$$

Elongation at break: R_2

$$R_2^{(D1)} = 26.101875 - 23.985\ X_1 - 30.715X_2 - 19.690X_3 - 217.08X_1X_2 + 54.08X_1X_3 - 41.12X_2X_3 - 16.885D_1X_1 - 1.715D_1X_2 + 6.889\ D_1X_3 \quad (7)$$

$$R_2^{(D2)} = 26.101875 - 23.985\ X_1 - 30.715X_2 - 19.690X_3 - 217.08X_1X_2 + 54.08X_1X_3 - 41.12X_2X_3 + 28.405D_2X_1 - 3.795D_2X_2 + 10.680\ D_2X_3 \quad (8)$$

$$R_2^{(D3)} = 26.101875 - 23.985\ X_1 - 30.715X_2 - 19.690X_3 - 217.08X_1X_2 + 54.08X_1X_3 - 41.12X_2X_3 - 5.315D_3X_1 - 14.485D_3X_2 - 4.809\ D_3X_3 \quad (9)$$

$$R_2^{(D4)} = 26.101875 - 23.985\ X_1 - 30.715X_2 - 19.690X_3 - 217.08X_1X_2 + 54.08X_1X_3 - 41.12X_2X_3 + 16.835D_4X_1 - 16.565D_4X_2 - 12.760\ D_4X_3 \quad (10)$$

Opacity: R_3

$$R_3^{(D1)} = 14.5503125 + 13.0525\ X_1 + 10.8475\ X_2 + 4.3975\ X_3 - 11.62X_1X_3 - 8.42X_2X_3 - 3.597D_1X_1 - 8.905D_1X_2 - 2.447\ D_1X_3 \quad (11)$$

$$R_3^{(D2)} = 14.5503125 + 13.0525\ X_1 + 10.8475\ X_2 + 4.3975\ X_3 - 11.62X_1X_3 - 8.42X_2X_3 + 8.507D_2X_1 - 4.995D_2X_2 - 3.557\ D_2X_3 \quad (12)$$

$$R_3^{(D3)} = 14.5503125 + 13.0525\ X_1 + 10.8475\ X_2 + 4.3975\ X_3 - 11.62X_1X_3 - 8.42X_2X_3 - 4.752D_3X_1 - 2.853D_3X_2 - 0.497\ D_3X_3 \quad (13)$$

$$R_3^{(D4)} = 14.5503125 + 13.0525\ X_1 + 10.8475\ X_2 + 4.3975\ X_3 - 11.62X_1X_3 - 8.42X_2X_3 - 7.352D_4X_1 - 16.747D_4X_2 + 6.502D_4X_3 \quad (14)$$

Where :

X_1 = mass of CNF-Raw (g)

X_2 = mass of CNF-Alkaline (g)

X_3 = mass of CNC (g)

D_i= indicator variable associated with the polymer matrix (D_1 = Oxpot ;D_2 = Oxyam ;D_3 = Oxcas ; and D_4 = Oxcor)

Statistical Analysis and Identification of Significant Effects on Responses R_1, R_2, and R_3

For each polynomial model, an analysis of the estimated coefficients and the associated probability values (Prob > |t|) presented in Tables 3, 4, and 5 allowed us to assess the statistical representativeness of the model.

An analysis of Tables 3, 4, and 5 shows that only the statistically significant coefficient estimates, along with their associated probabilities (Prob. > |t|), were retained. The resulting simplified models (equations 15,16 and 17) include only the significant main effects and interactions : $R_1(D_2)$, $R_2(D_2)$, and

$$R_1^{(D2)} : 69{,}072 + 72{,}425X_1 + 80{,}075X_2 + 66{,}075X_3 - 610{,}2X_1X_2 + 82{,}875D_2X_1 \quad (15)$$

$$R_2^{(D2)} : 26{,}102 - 30{,}715X_2 - 217{,}08X_1X_2 - 23{,}985X_1 + 28{,}405D_2X_1 \quad (16)$$

$$R_3^{(D2)} : 14{,}550 + 13{,}053\ X_1 + 10{,}848X_2 - 1{,}150X_1X_2 + 8{,}507D_2X_1 \quad (17)$$

ANOVA Analysis of Selected Responses

The results of the ANOVA analysis for the responses R_1 (strength at break), R_2 (elongation at break), and R_3 (opacity) are presented in Tables 6, 7, and 8. The analysis shows that the models (equations 15,16 and 17) are statistically significant ($p < 0.05$) with high F-values. The observed coefficients of determination (R^2 = 0.82–0.89; adjusted R^2 = 0.83–0.90) indicate that the experimental factors explain most of the observed variance. The residual errors (RMSE < 2.2) remain low relative to the response means, thus confirming the accuracy of the models. The results demonstrate that the nature and treatment of the reinforcements significantly influence the properties of the bioplastics. Breaking stress and elongation at break are particularly sensitive to interactions between factors, while opacity reflects the combined effect of the treatments on the matrix and the fibers. These models allow for the estimation of the final properties of the bioplastic. Robustness and statistical significance confirm the validity of the applied full factorial design. The simplified models, based on significant main effects and key interactions, robustly explain the variability in the responses. The matrix (D_2) (Oxyam), through the $D_2 \times X_1$ interaction, plays a decisive role in improving mechanical and optical performance, which allows for the identification of the most effective combinations of fibers and matrix for the development of functional bioplastics.

Interpretation of the Selected Responses

A joint analysis of the responses R_1(strength at break), R_2 (elongation at break), and R_3 (opacity) reveals the combined effect of the reinforcements $X_{1\,2}$ (CNF-Raw), X_2 (CNF-Alkaline), and X_3 (CNC), as well as their interactions. For R_2, all three reinforcements have a positive effect on strength at break, which could indicate that they improve the film's mechanical strength. However, the X_1X_2 interaction exhibits a significant negative effect, suggesting that a high combination of these two fibers could reduce mechanical performance. The $D_2 \times X_1$ interaction is positive, showing that when using the D_2 matrix, an increase in the X_1 factor improves the stress. For R_2,

Table 1 : Scope of the study

Factors	Designation	Type	Coded Level	Real Value / Modality
X_1	$m_{CNF\text{-}Raw}$ (g)	Continuous	–1 / +1	0 ; 0.25
X_2	$m_{CNF\text{-}Alkaline}$(g)	Continuous	–1 / +1	0 ; 0.25
X_3	m_{CNC}(g)	Continuous	–1 / +1	0 ; 0.25
D_i^*	Matrix type	Categorical		D_1;D_2;D_3;D_4

Table 2 : BioplasticsTesting Matrix

Run	Di : Matrix	X_1 : CFN_Rawmass (g)	X_2 : CFN_Alkaline mass (g)	X_3 : Mass CNC (g)	R_1 (MPa)	R_2 (%)	R_3 (%)
1	D_2 (OXYAM)	0.25	0.25	0.25	74.8	24.5	16.9
2	D_4 (OXCOR)	0.25	0	0	63.4	29.4	14.1
3	D_1 (OXPOT)	0	0.25	0	71.3	25.5	15
4	D_3 (OXCAS)	0.25	0.25	0.25	86.2	19.85	16.3
5	D_1 (OXPOT)	0	0.25	0.25	88.5	18.9	16.8
6	D_3 (OXCAS)	0.25	0.25	0	51.5	32.6	14.1
7	D_2(OXYAM)	0	0	0	17	45	6.5
8	D_1 (OXPOT)	0	0	0	16.3	42.5	7.6
9	D_4 (OXCOR)	0	0	0.25	48.6	44.2	10.1
10	D_4 (OXCOR)	0	0	0	25	38	12.5
11	D_2 (OXPOT)	0.25	0.25	0	80.3	20.15	17.4
12	D_2(OXYAM)	0	0.25	0	82.7	20.3	16.1
13	D_3 (OXCAS)	0	0.25	0	74.8	22.35	10.9
14	D_4 (OXCOR)	0.25	0.25	0	69.1	29.35	15.8
15	D_3 (OXCAS)	0	0.25	0.25	79.6	21.45	15.4
16	D_3 (OXCAS)	0	0	0.25	84.2	19.6	18
17	D_2 (OXYAM)	0.25	0	0.25	64.9	30.85	15
18	D_1 (OXPOT)	0.25	0	0.25	88.7	18.4	17.1
19	D_2(OXYAM)	0.25	0	0	68.9	27.8	14.75
20	D_2(OXYAM)	0	0.25	0.25	67.8	27.4	12.2
21	D_2(OXYAM)	0.25	0.25	0	82.7	20.3	16.1
22	D_3 (OXCAS)	0.25	0	0	76.9	21.1	16.7
23	D_4 (OXCOR)	0	0.25	0.25	92.5	16.95	17.6
24	D_4 (OXCOR)	0.25	0	0.25	90.6	17.6	17.2
25	D_1 (OXPOT)	0	0	0.25	71.7	7.85	8.3
26	D_2 (OXYAM)	0.25	0	0	95.3	17.06	17.56
27	D_4 (OXCOR)	0.25	0.25	0.25	81.6	15.6	16.8
28	D_1 (OXPOT)	0	0	0.25	22.5	40	7.8
29	D_3 (OXCAS)	0.25	0	0.25	72.5	26.2	15.4
30	D_4 (OXCOR)	0	0.25	0	79.3	11.1	16.4
31	D_3 (OXCAS)	0	0	0	18.5	43.5	12.5
32	D_1 (OXPOT)	0.25	0.25	0.25	69.6	12.9	11.7

Table 3 : Estimation of coefficients and (Prob > ltl) for the set of responses R_1

Term	Coefficient Estimate	(Prob > ltl)	Significance
Intercept	69.071875	<0.0001	Significant
X_{1^2}	72.425	0.0167	Significant
X_2	80.075	0.0096	Significant
X_{2^2}	66.075	0.0264	Significant
X_1X_2	-610.2	0.012	Significant
X_1X_3	-233.4	0.214	Not significant
X_2X_3	-201	0.009	Significant
D_1X_1	-40.325	0.284	Not significant
$D_{1^2}X_{2^2}$	-14.575	0.3936	Not significant
$D_{1^2}X_3$	-18.175	0.3701	Not significant
$D_{2^2}X_{1^2}$	82.875	0.0329	Significant
D_2X_2	26.825	0.5673	Not significant
D_2X_3	-39.975	0.5531	Not significant
D_3X_1	-0.125	0.9979	Not significant
D_2X_2	27.825	0.6168	Not significant
D_3X_3	23.425	0.4609	Not significant
D_4X_1	-42.425	0.2889	Not significant
D_4X_2	-40.075	0.3583	Not significant
D_4X_3	-40.075	0.3583	Not significant

Table 4 : Estimation of coefficients and (Prob > ltl) for the set of responses R_2

Term	Coefficient Estimate	(Prob > ltl)	Significance
Intercept	26.101875	<0.0001	Significant
X_{1^2}	-23.985	0.0289	Significant
X_2	-30.715	0.0200	Significant
X_3	-19.690	0.113	Not significant
X_1X_2	-217.08	0.148	Not significant
X_1X_3	54.08	0.021	Significant
$X_2X_{2^2}$	-41.12	0.117	Not significant
D_1X_1	-16.885	0.4153	Not significant
D_1X_2	-1.715	0.4153	Not significant
D_1X_3	6.889	0.4153	Not significant
D_2X_1	-28.405	0.1805	Not significant
D_2X_2	-3.795	0.1805	Not significant
D_2X_3	10.680	0.1805	Not significant
D_3X_1	-5.315	0.7953	Not significant
D_3X_2	-14.485	0.4167	Not significant
D_3X_2	-4.809	0.4240	Not significant
D_4X_1	16.835	0.0358	Significant
D_4X_2	-16.565	0.7368	Not significant
D_4X_3	-12.760	0.6646	Not significant

the X_1 and X_2 reinforcements have a negative effect on the elongation at break, meaning they increase the material's stiffness and reduce its deformation capacity. This stiffening is further accentuated by the X_1X_2 interaction. However, the $D_1 \times X_2$ interaction is positive and significant, indicating that using the Oxyam matrix reinforced with X_1 reduces the stiffness of the bioplastic films. This effect helps limit excessive stiffness and maintain a certain degree of ductility in the bioplastic. Thus, thanks to this

Fig. 1: Photograph of the CNF-Raw reinforcement

Fig. 2: Photograph of the CNF -Alkaline reinforcement

interaction, the bioplastic exhibits a better balance between stiffness and ductility, which reduces the risk of material brittleness. For R_3, the X_1 (CNF-Raw) and X_2 (CNF-Alkaline) fibers have a positive and significant effect on R_3. These observed effects could mean that they contribute to making the film more opaque. However, the slightly negative X_1X_2 interaction suggests that a strong combination of the two fibers does not make the film even more opaque. These observed negative interactions could be explained by "saturation" effects or competition for space within the matrix, i.e., the fibers overlap or stack on top of one another, which slightly reduces the expected effect on opacity. The observed positive and significant $D_2 \times X_1$ interaction could mean that the Oxyam matrix, consisting of dietary fibers such as cellulose, hemicellulose, and lignin, enhances the effect of X_1, thereby improving light scattering and thus the film's opacity.

Table 5: Estimated coefficients and (Prob > ltl) for all R_3 responses

Term	Coefficient Estimate	(Prob > ltl)	Significance
Intercept	14.550313	<0.0001	Significant
X_{1^2}	13.0525	0.0004	Significant
X_2	10.8475	0.0019	Significant
X_{2^2}	4.3975	0.1406	Not significant
X_1X_2	-11.62	0.041	Significant
X_1X_3	-11.62	0.173	Not significant
X_2X_3	-8.42	0.041	Significant
D_1X_1	-3.597	0.4718	Not significant
$D_{1^2}X_{2^2}$	-8.905	0.4766	Not significant
$D_{1^2}X_3$	-2.447	0.9199	Not significant
$D_{2^2}X_{1^2}$	8.507	0.0026	Significant
D_2X_2	-4.995	0.3225	Not significant
D_2X_3	-3.557	0.5668	Not significant
D_3X_1	-4.752	0.2033	Not significant
D_2X_2	-2.853	0.6130	Not significant
D_3X_3	-0.497	0.7133	Not significant
D_4X_1	-7.352	0.0043	Significant
D_4X_2	-16.747	0.0059	Significant
D_4X_3	6.502	0.2033	Not significant

Bioplastics in the Study

Based on the preceding sections regarding the experimental matrix, statistical analysis, and identification of significant effects on the responses R_1, R_2, and R_3, trial 26 of the experimental matrix presents the best compromise between the mechanical and optical properties of the bioplastic films. The values obtained for R_1, R_2, and R_3 (95.3 MPa, 17.06%, and 17.56%, respectively) indicate a satisfactory balance between mechanical strength, ductility, and opacity. This performance could be explained by the $D_2 \times X_1$ interaction, corresponding to the Oxyam matrix (D_2) and the CNF-Raw (X_1), which promotes fiber–matrix compatibility as well as interfacial adhesion and load transfer within the polymer network. Similar results were observed

Table 6: ANOVA of R_1 (Breaking Strength)

Source	DF	SS	MS	F-value	(Prob > ltl)	R_2	Adjusted R_2	RMSE Response	Mean	N
Model	18	312.450	17.358	4.412	0.0056	0.8186	0.8489	2.0487	69.072	32
Residual	13	51.185	3.937							
Corrected Total	31	363.635								

Table 7: ANOVA of R_1 (Elongation at break)

Source	DF	SS	MS	F-value	(Prob > ltl)	R_2	Adjusted R_2	RMSE Response	Mean	N
Model	18	192.4672	10.6926	3.2145	0.0123	0.8123	0.8324	2.1043	26.102	32
Residual	13	43.3241	3.3326							
Corrected Total	31	235.7913								

Table 8: ANOVA of R_1 (Opacity)

Source	DF	SS	MS	F-value	(Prob > ltl)	R_2	Adjusted R_2	RMSE Response	Mean	N
Model	18	286.08281	15.8935	4.0471	0.0068	0.8886	0.9019	1.9817	14.550	32
Residual	13	51.05229	3.9271							
Corrected Total	31	337.13510								

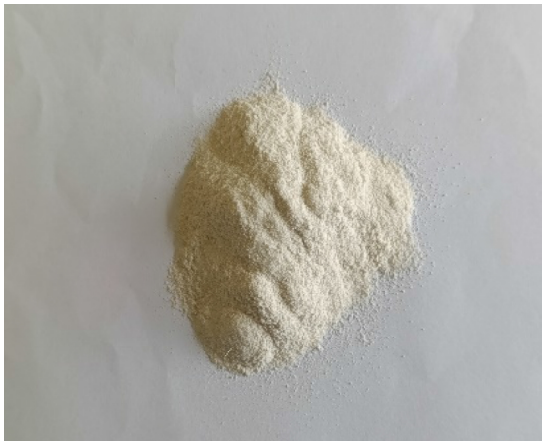

Fig. 3: Photograph of CNC reinforcements

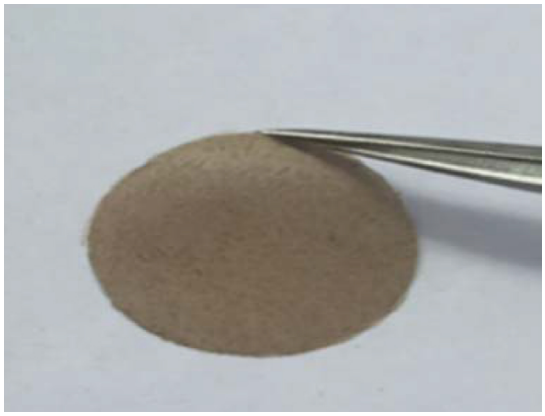

Fig. 5: Photograph of TPS bioplastics

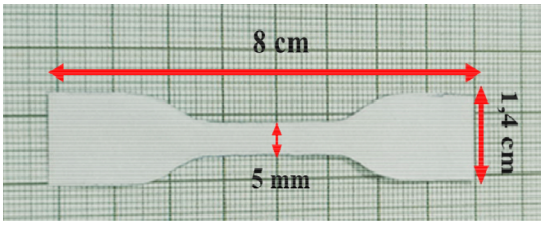

Fig. 4: Type IV (D-638) dumbbell-shaped test specimens

by Abdul Karim et al. (2021)[12] and Permatasari et al. (2022)[13], who used full factorial designs to optimize the formulation and identify the interactions influencing mechanical properties. The resulting bioplastic is designated TPS (Thermoplastic Starch), and its macroscopic appearance is shown in Figure 5.

SEM Morphology

The results of the SEM analysis, shown in Figure 6, reveal that the internal structure of the TPS film exhibits several morphological defects. Microcracks (Fig. 6a) and discontinuities (Fig. 6b) are observed in the matrix, indicating a certain degree of heterogeneity in the TPS bioplastic. These defects, although scattered, may indicate weak interfacial cohesion and/or high internal stresses during drying, leading to structural fragility. The presence of these irregularities could constitute local areas of weakness capable of influencing the structural

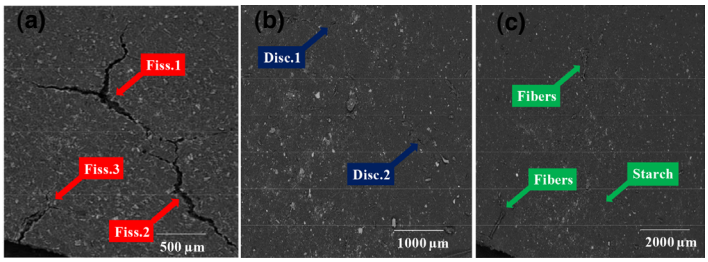

Fig. 6: SEM micrographs of the TPS film

stability of the bioplastic. Thus, the observed microstructure highlights certain limitations related to the film's internal organization.

CONCLUSION

This study demonstrated the value of experimental design methodology, particularly the mixed full factorial design, for the study of starch-based bioplastics reinforced with fillers. Analysis of the simplified models (equations 15, 16, and 17) indicated that the factors X_1, X_2, and X_3, as well as the interaction $D_2 \times X_1$, significantly influence tensile strength, elongation at break, and opacity, regardless of the response obtained. The results also showed that Test 26 presents a satisfactory compromise between the mechanical and optical properties of the ATP film. Furthermore, SEM analysis revealed the presence of microcracks and scattered, unconnected discontinuities, indicating certain irregularities in the film's internal structure. Overall, these observations highlighted the key factors and interactions that must be taken into account to understand the material's behavior.

ACKNOWLEDGMENTS

We extend our sincere thanks to the Nangui ABROGOUA University Central Laboratoryand toPeleforoGON COULIBALY University and the Water and Environment Laboratory Limoges E2Lim, UR 24133, ENSIL-ENSCI, University of Limoges, France, for their invaluable technical support, which was crucial to the success of this work.

Conflict of Interest

The authors declare that they have no conflict of interest related to this manuscript.

Funding Declaration

The authors declare that they have not received any funding from any third party (government agency, commercial entity, or private foundation) for the completion of this article.

Author Contributions

Ouattara Taniky Sy Hamed: Original manuscript drafting, writing, data management, software, visualization, conceptualization, methodology

Yacouba Zoungranan:Formal analysis, Writing, Original draft preparation, Visualization
Sévérin N'goran Eroi :Data management, software, visualization,
Ekou Lynda: Conceptualization, methodology
Ekou Tchirioua: Supervision, validation
Kaga Taba To'ora: Survey, visualization

Data Availability Statement

Data are available and can be provided upon request.

Ethical Approval Statement

All authors involved in this study fully consent to its publication. Furthermore, this research did not involve the use of animals at any stage of the experimental process.

Informed Consent Statement

All individuals listed as authors in this article have read its content and approve its submission for publication.

REFERENCES

1. Jiao, H.; Ali, S. S.;Alsharbaty, M. H. M.;Elsamahy, T.; Abdelkarim, E.;Schagerl, M.; Al-Tohamy, R.; Sun, J.. EcotoxicolEnvironSaf2024;271:115942 ,Doi: 10.1016/j.ecoenv.2024.115942.
2. Dos Muchangos, L. S.; Ito, L.; Tokai, A.. *J Mater Cycles Waste Manag* **2025**; *27*:624–637, Doi: 10.1007/s10163-024-02098-z.
3. Goh, S. L.; Yap, K. S.; Neo, E. R. K.; *et al..Waste Manag* **2025**; *200*:114760, Doi: 10.1016/j.wasman.2025.114760.
4. Keyes, A.; Saffron, C. M.;Manjure, S.; Narayan, R..*Polymers* **2024**;*16(21)*:3073, Doi: 10.3390/polym16213073.
5. Muhammad, A.; Rashidi, A. R.; Buddin, M. M. H.. *Int J Eng Technol* **2018**;*7(4.18):* 267–270, Doi: 10.14419/ijet.v7i4.18.21932.
6. Olusanya, J.; Mohan, T. P.; Kanny, K.. *J Polym Res* **2023**;*30*:262, Doi: 10.1007/s10965-023-03646-1.
7. Hamed, O. T. S.; Zoungranan, Y.; Lynda,

E.; Tchirioua, E. *Indian J Sci Technol* **2025***;18(6):*452–463, Doi: 10.17485/ijst/v18i6.3736.
8. Habibi, Y.; Lucia, L. A.; Rojas, O. *J. Chem Rev* **2010**;*110(6):*3479–3500, Doi: 10.1021/cr900339w.
9. Dufresne, A.. *Mater Today* **2013***;16(6):*220–227, Doi: 10.1016/j.mattod.2013.06.004.
10. Abd Karim, S. F.; Idris, J.; Jai, J.; Musa, M.; Ku Hamid, K. H.. *Polymers* **2022**;*14(19),* Doi: 10.3390/polym14194213.
11. Permatasari, N. D.; Witoyo, J. E.; Masruri, M.; Yuwono, S. S.; Widjanarko, S. B. Nat *Environ Pollut Technol* **2022**; *21(4):*1893–1901, Doi: 10.46488/nept.2022.v21i04.044.
12. Abd Karim, S. F.; Idris, J.; Jai, J.; Musa, M.; Ku Hamid, K. H. *Polymers* **2021**;*14(19),* Doi: 10.3390/polym14194213.
13. Permatasari, N. D.; Witoyo, J. E.; Masruri, M.; Yuwono, S. S.; Widjanarko, S. B. *Nat EnvironPollut Technol* **2022**; *21(4):*1573–1580, Doi: 10.46488/NEPT.2022.v21i04.044.